

# Evaluation of Non-Staggered Body-Fitted Grid Based Solution Method in Application to Supercritical Fluid Flows

Suresh Sahu, Abhijeet M. Vaidya, Naresh K. Maheshwari

**Abstract**—The efforts to understand the heat transfer behavior of supercritical water in supercritical water cooled reactor (SCWR) are ongoing worldwide to fulfill the future energy demand. The higher thermal efficiency of these reactors compared to a conventional nuclear reactor is one of the driving forces for attracting the attention of nuclear scientists. In this work, a solution procedure has been described for solving supercritical fluid flow problems in complex geometries. The solution procedure is based on non-staggered grid. All governing equations are discretized by finite volume method (FVM) in curvilinear coordinate system. Convective terms are discretized by first-order upwind scheme and central difference approximation has been used to discretize the diffusive parts.  $k-\epsilon$  turbulence model with standard wall function has been employed. SIMPLE solution procedure has been implemented for the curvilinear coordinate system. Based on this solution method, 3-D Computational Fluid Dynamics (CFD) code has been developed. In order to demonstrate the capability of this CFD code in supercritical fluid flows, heat transfer to supercritical water in circular tubes has been considered as a test problem. Results obtained by code have been compared with experimental results reported in literature.

**Keywords**—Curvilinear coordinate, body-fitted mesh, momentum interpolation, non-staggered grid, supercritical fluids.

## I. INTRODUCTION

To fulfill the future energy demand, Generation-IV International Forum (GIF) is developing next generation nuclear energy system. The main objectives of GIF are to use fuel more efficiently, high level of safety, reduce waste production, and to be economically competitive [1]. To meet the above mentioned objectives, GIF has recommended six most promising reactor concepts. SCWR is one of them. SCWR has higher thermal efficiency compared to conventional nuclear reactors. In addition, simple plant design and low capital and operation cost are some other benefits that make SCWR more promising.

A fluid is in the supercritical state when it is subjected to pressure and temperature higher than its critical value. For water the critical pressure and temperature are 221.15 bar and 374.15 °C, respectively. At supercritical pressure, fluid remains at single phase and under certain condition they undergo large property variation. Fig. 1 shows the variation of thermo-physical properties of water near pseudo-critical temperature at 245 bar. For a particular pressure, pseudo-critical temperature of any fluid is defined by the temperature

at which specific heat attains a maximum values. This strong property variation at supercritical pressure has a strong bearing on the heat transfer phenomena. So the detailed understanding of this phenomenon is essential which will be useful for SCWR design.

Research on heat transfer to supercritical fluid is still in progress worldwide. Majority of experiments have been performed in tube using water or carbon dioxide as working fluid. The existing experimental and theoretical studies on heat transfer at supercritical pressure have been reviewed and published by several authors [2]-[4]. In most of the SCWR design concepts [5], [6], reactor core is grouped into several zones where supercritical water flows in vertical/horizontal, upward/downward directions. Yamagata et al. [7] performed experimental studies on heat transfer to supercritical water flowing in horizontal and vertical circular tubes. Zhao et al. [8] focused on vertically downward flow in tube. Zhang et al. [9] did experiments using Freon (R-134a) as a working fluid in a circular tube. Similarly Mori et al. [10] studied heat transfer to supercritical pressure fluid flowing vertically upward and downward in tube using R-22 as working fluid. Computational approach has been also adopted by some researchers. CFD commercial software Fluent has been used by Zhang et al. [11] to study the heat transfer behavior in of supercritical fluids in vertical and horizontal tubes. Similarly Jaromin et al. [12] used ANSYS-CFX code for the analysis in vertical tube. Wen et al. [13] numerically investigated the heat transfer deterioration phenomenon in vertical tubes.

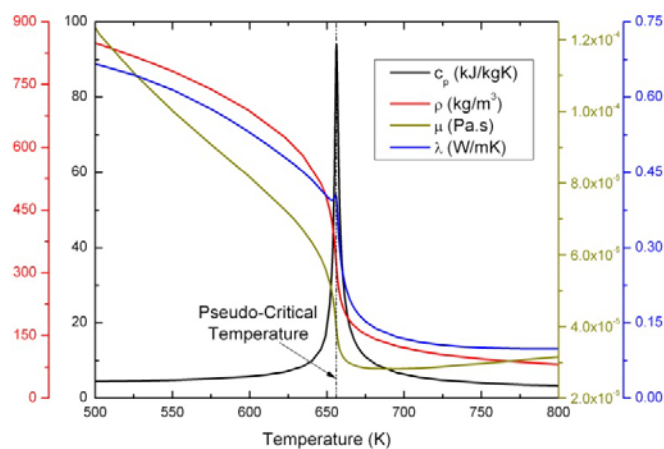


Fig. 1 Variation of thermo-physical properties of water near pseudo-critical temperature at 245 bar

Suresh Sahu is with the Homi Bhabha National Institute, India (e-mail: ssureshiitg@gmail.com).

CFD is an important tool for better understanding the behavior of fluid flow and heat transfer in engineering systems. Many engineering applications e.g. automobile, nuclear reactor, aerospace, etc. involve complex geometries. Body-fitted coordinate (BFC), in which coordinate lines follow the boundary of the geometry, can handle these complex geometries very well. Using multi-block concept, this method can generate more complex geometries. The objective of the present work is to evaluate the body-fitted grid based solution method in the context of supercritical fluid flows. For computing flows in BFC, conservation equations have been transformed from physical coordinate system  $(x, y, z)$  to computational coordinate system  $(\xi, \eta, z)$  using chain rule. These transformed conservation equations have been discretised by control volume based discretization method. The transformed equation is integrated over a control-volume and then discretized [14]-[16]. The solution method is based on non-staggered grid [17], [18] in which all the variables are stored at cell centre. Momentum interpolation method given by Rhie and Chow [19] has been adopted for cell face velocity computation. The coupling between mass and momentum equation has been done by SIMPLE algorithm by properly formulating for non-orthogonal curvilinear grid. In order to handle turbulent flows, standard  $k - \varepsilon$  model [20] with standard wall function has been implemented over curvilinear coordinates. The solution method has been reported in detail in section 'Numerical Modelling'.

In order to validate the results obtained by body-fitted grid based solver, the experimental results reported by Yamagata et al. [7] have been selected for comparison. Simulations have been performed for vertically upward flow in pipe using water as a working fluid. After validation of the solver, simulations have been performed for various heat flux, mass flux and pressure. The analysis has been done on the basis of the variation of wall temperature and Nusselt number with bulk mean enthalpy of the fluid.

## II. NUMERICAL MODELLING

The formulation of the present solution method is developed under the assumption that the flow is steady, variable property, incompressible and turbulent. The present solver solves for the Reynolds averaged continuity, Navier-Stokes equations and temperature based energy equation. For handling turbulent flows, it solves for equations for turbulent kinetic energy ( $k$ ) and its dissipation rate ( $\varepsilon$ ). All governing equations can be expressed by single scalar transport equation. For general dependent variable ( $\phi$ ) it can be written in the Cartesian coordinate system as follows:

$$\frac{\partial}{\partial x}(\rho u \phi) + \frac{\partial}{\partial y}(\rho v \phi) + \frac{\partial}{\partial z}(\rho w \phi) = \frac{\partial}{\partial x} \left( \Gamma_{\phi} \frac{\partial \phi}{\partial x} \right) + \frac{\partial}{\partial y} \left( \Gamma_{\phi} \frac{\partial \phi}{\partial y} \right) + \frac{\partial}{\partial z} \left( \Gamma_{\phi} \frac{\partial \phi}{\partial z} \right) + S_{\phi} \quad (1)$$

$u, v, w$  are time-averaged velocities in  $x, y, z$  directions respectively.  $\Gamma_{\phi}$  and  $S_{\phi}$  are the corresponding diffusion coefficients and source terms respectively for the general dependent variable ( $\phi$ ). All the governing equations can be derived by properly defining the terms  $\phi, \Gamma_{\phi}$  and  $S_{\phi}$ . For example, the continuity equation can be derived by defining  $\phi$  as 1 and  $\Gamma_{\phi}$  and  $S_{\phi}$  as 0.

The present solution method is based on BFC system. In this method, complex shaped physical domain is transformed into simple rectangular computation domain by curvilinear BFC system. Hence, it is necessary to transform all the governing equations from Cartesian coordinate system to BFC system. This coordinate transformation is done by chain rule. Ultimate objective of present work is to develop a CFD code for nuclear rod bundles. Nuclear rod bundles can be imagined as a big cylinder containing a number of co-axial small cylinders with an inlet and outlet. For handling such kind of geometries, full 3-D transformation is not needed, only cross-section ( $x$ - $y$  plane) is mapped by body fitted grid and this cross-sectional mesh is extruded in the axial direction to get 3-D mesh. Transformation of physical domain into computation domain is illustrated in Fig. 2.

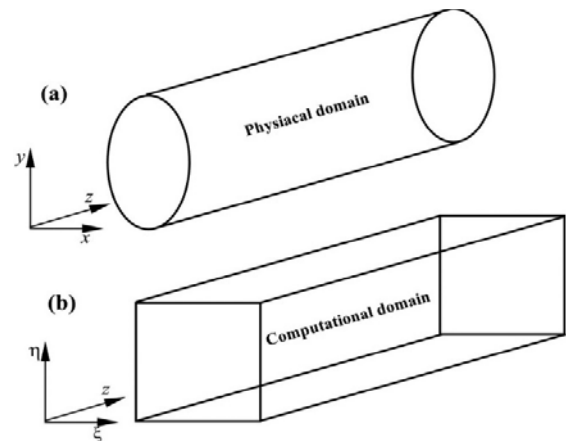


Fig. 2 Transformation of (a) physical domain (in Cartesian coordinates) into (b) computational domain (BFC)

Transformation of  $x$ - $y$  plane takes place by introducing curvilinear coordinates  $\xi = \xi(x, y)$  and  $\eta = \eta(x, y)$ . Using chain rule, (1) can be transformed from  $(x, y, z)$  to  $(\xi, \eta, z)$  coordinate system and the same can be written as follows:

$$\frac{\partial}{\partial \xi}(\rho U \phi) + \frac{\partial}{\partial \eta}(\rho V \phi) + \frac{\partial}{\partial z}(\rho w \phi) = \frac{\partial}{\partial \xi} \left[ C_1 \left( \Gamma_{\phi} \frac{\partial \phi}{\partial \xi} \right) + C_2 \left( \Gamma_{\phi} \frac{\partial \phi}{\partial \eta} \right) \right] + \frac{\partial}{\partial \eta} \left[ C_3 \left( \Gamma_{\phi} \frac{\partial \phi}{\partial \xi} \right) + C_4 \left( \Gamma_{\phi} \frac{\partial \phi}{\partial \eta} \right) \right] + \frac{\partial}{\partial z} \left( \Gamma_{\phi} \frac{\partial \phi}{\partial z} \right) + S_{\phi}(\xi, \eta, z) \quad (2)$$

In the above equation,  $U$  and  $V$  are contravariant velocity components given by the following expressions:

$$U = u\xi_x + v\xi_y; V = u\eta_x + v\eta_y \quad (3)$$

and  $C_1, C_2, C_3, C_4$  are geometric coefficients defined as:

$$C_1 = \xi_x^2 + \xi_y^2; C_4 = \eta_x^2 + \eta_y^2; C_2 = C_3 = \xi_x\eta_x + \xi_y\eta_y$$

$$\xi_x = \frac{y_\eta}{J}; \xi_y = -\frac{x_\eta}{J}; \eta_x = -\frac{y_\xi}{J}; \eta_y = \frac{x_\xi}{J};$$

$$J = x_\xi y_\eta - y_\xi x_\eta$$

$S_\phi$  is the transformed  $S_\phi$  terms and  $J$  is the Jacobian determinant.

All transformed governing equations have been discretized by FVM. The present solution technique uses Non-staggered grid in which all variables are stored at cell centres. Discretization of convective terms has been done by first-order upwind scheme and central difference scheme has been used for diffusive terms. In order to perform pressure-velocity coupling on non-staggered grid, Rhie and Chow momentum interpolation method [19] has been used to compute velocity components at cell faces and the SIMPLE algorithm is extended to curvilinear coordinate system.

In the present solver, governing equations are subjected to following boundary conditions: "INLET", "OUTLET" and "WALL". At the INLET boundary appropriate values of velocity components, temperature, turbulent kinetic energy and its dissipation rate are specified. At OUTLET boundary, only pressure is specified and all other dependent variables are extrapolated from the adjacent interior cell. On WALL boundary, the standard wall function originally proposed for orthogonal Cartesian coordinates has been implemented for non-orthogonal curvilinear BFC. For energy equation, constant heat flux has been specified at the WALL boundary. In order to handle the property variation of fluid (viscosity, thermal conductivity, density, specific heat and enthalpy) at supercritical pressure, properties as function of temperature are expressed in tabular form. The tabular form is capable of handling any type pattern. Piece-wise linear interpolation method has been adopted to find the property at intermediate temperature. NIST database has been used to evaluate thermo-physical properties of water at different pressure and temperature. The resulting sets of algebraic equations have been solved by alternating direction line by line TDMA method.

### III. RESULTS AND DISCUSSION

In order to access the capability of solution method at supercritical pressure, heat transfer analysis of upward flow of water in a vertical pipe is considered as a test problem. Pipe diameter is taken as 7.5 mm and length is adjusted for each heat flux such that bulk enthalpy varies from 1400 to 2800 kJ/kg. Simulations have been performed for pressure from 240

to 250 bar, mass flux from 800 to 1830 kg/m<sup>2</sup>s and heat flux from 233 to 698 kW/m<sup>2</sup>.

The computational results must be grid independent so several different grid sizes were made and tested. For grid independent study simulations have been performed for pressure of 245 bar, mass flux of 1260 kg/m<sup>2</sup>s and heat flux of 698 kW/m<sup>2</sup> for three different meshes. Mesh-A is coarse mesh with 21×21 cells at the cross-section of the pipe. Mesh-B is contains 31×31 cells and Mesh-C is fine mesh with 41×41 cells at the cross-section. In axial direction 800 nodes (uniform) have been taken for all three meshes. Fig. 3 shows the variation in wall temperature with respect to bulk mean enthalpy for all three meshes. For Mesh-B and Mesh-C, wall temperature variation is almost identical. Since the solver handles turbulent flows using standard  $k-\epsilon$  model, the success of computations is dependent on  $Y^+$  value. Variation of  $Y^+$  with respect to pipe length is shown in Fig. 4. For all three meshes,  $Y^+$  is greater than 11.63 over the entire pipe but for Mesh-C, the range of  $Y^+$  is very close to the limiting values. So with this study, it can be concluded that Mesh-C is considered to possess sufficient computational accuracy.

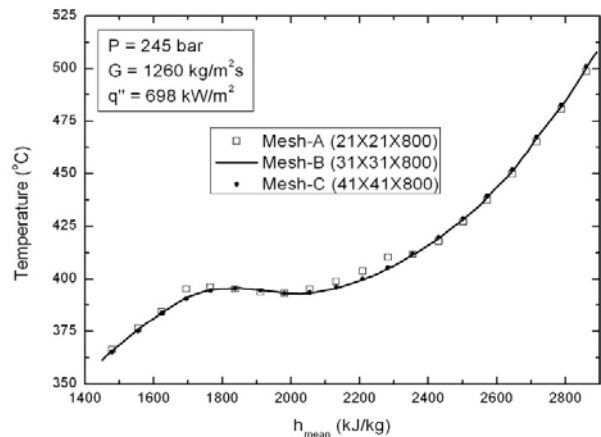


Fig. 3 Grid independent test: Variation of wall temperature with respect to bulk mean enthalpy

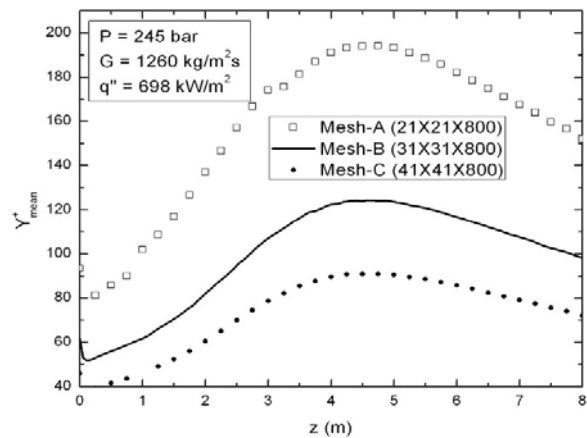


Fig. 4 Grid independent test: Variation of  $Y^+$  with respect to pipe length

Analysis of heat transfer is based on cross-sectional mean parameters like bulk mean temperature, bulk mean enthalpy, bulk mean velocity etc. The cross-sectional bulk mean temperature and velocities are calculated by mass weighted average. Based on these bulk mean temperature all thermo-physical properties are calculated from property table. Further, heat transfer analysis is carried out by cross-sectional averaged Nusselt number (Nu). It is defined as  $\alpha D_h / \lambda$ , where  $\alpha$  and  $\lambda$  are convective heat transfer coefficient and cross-sectional mean thermal conductivity respectively. Heat transfer coefficient is computed by following expression.

$$\alpha = \frac{q''}{T_{w_{mean}} - T_{mean}}$$

Average wall temperature ( $T_{w_{mean}}$ ) is calculated by averaging wall temperature data along the circumferential direction at certain axial location. Average wall temperature and mean fluid temperature ( $T_{mean}$ ) are calculated by following equations.

$$T_{w_{mean}} = \frac{\int_r T_w dl}{\int_r dl}; \quad T_{mean} = \frac{\int_{A_c} \rho w c_p T dA_c}{\int_{A_c} \rho w c_p dA_c}$$

Simulations have been performed for three different pressures, mass flux and heat flux. The test matrix of the present work is shown in Table I. For validation of the solution method and solver, the experimental results reported by Yamagata et al. [7] are considered as benchmark and comparison has been made between the results obtained by present solver and the one reported by Yamagata et al. [7].

TABLE I  
 TEST MATRIX IN THE PRESENT STUDY

Pressure-p (bar)	Mass flux-G (kg/m <sup>2</sup> s)	Heat flux- $q''$ (kW/m <sup>2</sup> )
240	1260	465
	800	698
245	1260	233 465 698
	1830	698
250	1260	465

The effect of heat flux, mass flux and pressure on supercritical water flowing upward in vertical pipe have been analyzed and it is reported in terms of Nusselt number and wall temperature variations with respect to bulk mean enthalpy. In general with increase in enthalpy Nusselt number increases and it reaches to its maximum value just before the pseudo-critical point and after that Nusselt number decreases with enthalpy. Wall temperature increases with increase in enthalpy. Near pseudo-critical point wall temperature is almost constant (for low heat flux) due to high specific heat

and after that with increase in enthalpy wall temperature increases.

#### A. Effect of Heat Flux

Fig. 5 shows the variation of average wall temperature and Nusselt number with bulk-mean enthalpy and heat flux at the pressure of 245 bar and mass flux of 1260 kg/m<sup>2</sup>s. From Fig. 5 (a) it is clear that average wall temperature increases with heat flux. Near the pseudo-critical point minimum temperature difference between two heat fluxes has been observed. The nearly constant wall temperature profile near pseudo-critical region gradually disappears with the increase of heat flux. Variation of bulk-mean temperature is also reported in Fig. 5 (a). For low heat flux, average wall temperature variation trend resembles closely to the trend of bulk-mean temperature but as heat flux increases wall temperature increases rapidly. For validation of solution method and code, average wall temperature variations reported by Yamagata et al. [7] have also been included in Fig. 5 (a). Slight deviation with benchmark result for high heat flux (698 kW/m<sup>2</sup>) near critical region is visible, suggesting that still finer mesh is required. Apart from that the code results are in good agreement with one reported by Yamagata et al. [7]. As shown in Fig. 5 (b), near the vicinity of pseudo-critical point, for lower heat flux, higher Nusselt number has been observed. For  $h < h_{pc}$ , Nusselt number is almost same for all heat fluxes. With increasing heat flux, peak value of Nusselt number shifts towards the lower bulk enthalpy value.

#### B. Effect of Mass Flux

Fig. 6 (a) shows the variation of average wall temperature with bulk-mean enthalpy and mass flux at the pressure of 245 bar and heat flux of 698 kW/m<sup>2</sup>. In general, with increase in mass flux, the average wall temperature decreases. This wall temperature decreasing trend is more rapid at low mass flux (800 to 1260 kg/m<sup>2</sup>s) compared to high mass flux (1260 to 1830 kg/m<sup>2</sup>s). The lower temperature difference between the wall and bulk-fluid at high mass flux compared to that at low mass flux, suggests that the Nusselt number for high mass flux is higher compared to low mass flux. The same trend has been shown in Fig. 6 (b). Apart from pseudo-critical region, the effect of mass flux on Nusselt number appears in low as well as high bulk-mean enthalpy regions, which has not been observed in Fig. 5 (b) (in which the effect of heat flux is studied).

#### C. Effect of Pressure

In order to understand the effect of pressure, simulations have been performed for pressures of 240, 245 and 250 bar. Fig. 7 illustrates the variation of average wall temperature and Nusselt number plotted against the bulk-mean enthalpy at heat flux of 465 kW/m<sup>2</sup> and mass flux of 1260 kg/m<sup>2</sup>s. From Fig. 7 (a) it is clear that, at low mean enthalpy region, wall temperature variations are almost identical for all three pressures. Near pseudo-critical region and high enthalpy region higher wall temperature has been observed for higher pressure. The effect of pressure on Nusselt number is not

significant in low and high bulk enthalpy region. It appears only in pseudo-critical region where higher Nusselt number has been observed for lower pressure.

#### IV. CONCLUSIONS

In the present work, a 3-D non-staggered body-fitted grid based solution method for fluid flow and heat transfer analysis has been explained. In order to investigate the capability of the present solver in predicting the heat transfer phenomena in circular pipe at supercritical pressures, the relevant experimental data were selected from literature [7]. The results obtained by solver are very close to the same reported in benchmark experimental work. The variation of average wall temperature and Nusselt number against bulk mean enthalpy for various heat flux, mass flux and pressure are qualitatively same as that of reported in reviewed literatures. The exercise indicates that the present solution method is capable of solving fluid flows and heat transfer problems in supercritical pressure condition.

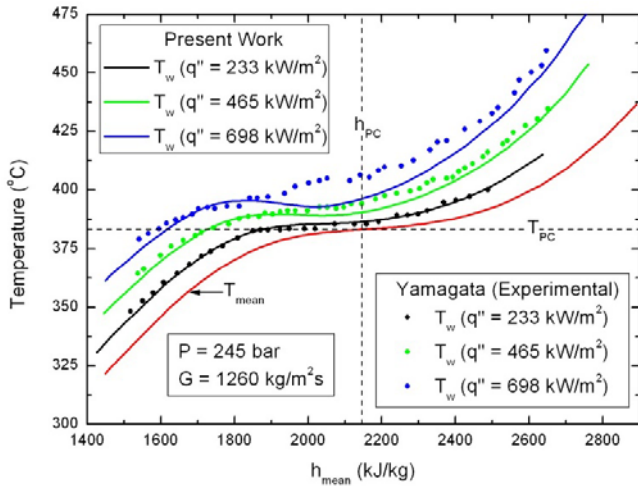


Fig. 5 (a) Effect of heat flux: Variation of average wall temperature with respect to bulk-mean enthalpy

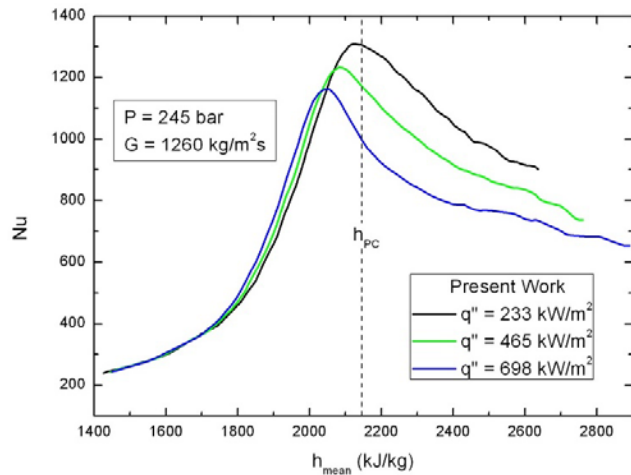


Fig. 5 (b) Effect of heat flux: Variation of Nusselt number with respect to bulk-mean enthalpy.

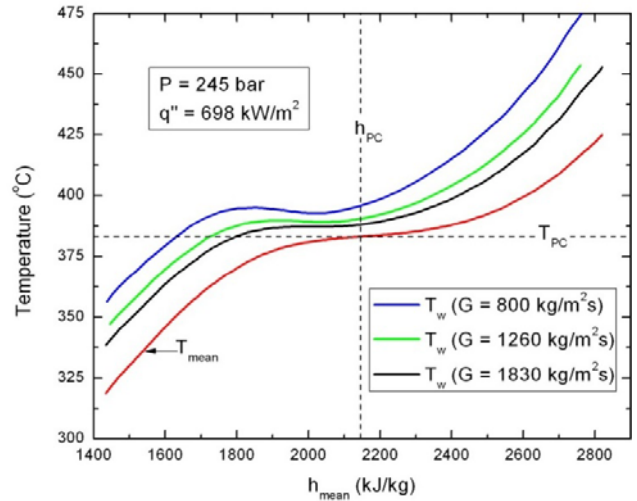


Fig. 6 (a) Effect of heat flux: Variation of average wall temperature with respect to bulk-mean enthalpy

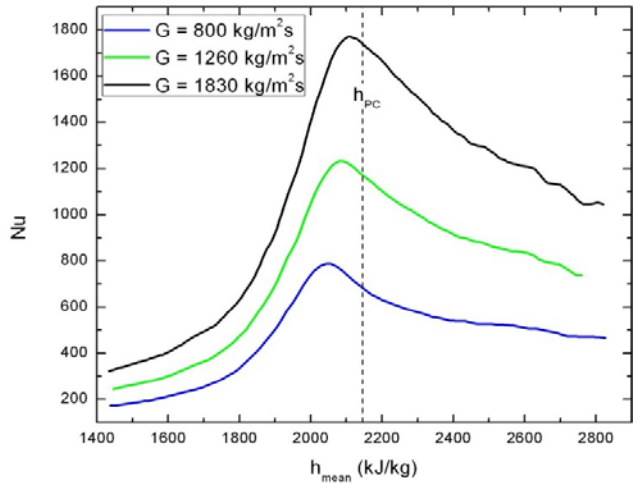


Fig. 6 (b) Effect of mass flux: Variation of Nusselt number with respect to bulk-mean enthalpy

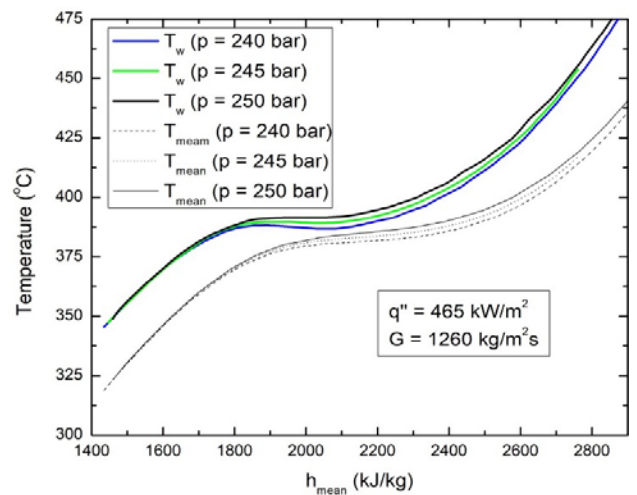


Fig. 7 (a) Effect of pressure: Variation of average wall temperature with respect to bulk-mean enthalpy

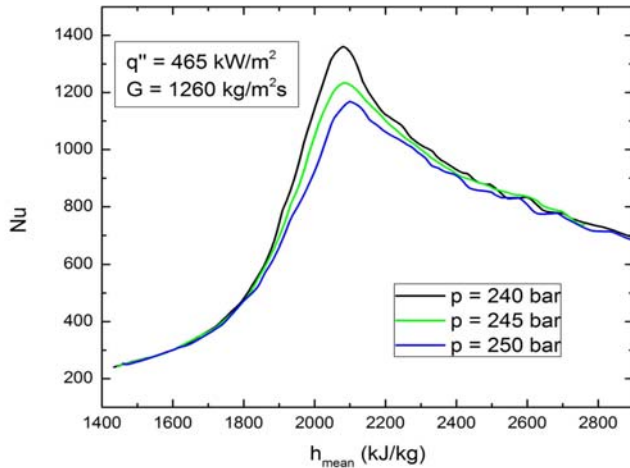


Fig. 7 (b) Effect of mass flux: Variation of Nusselt number with respect to bulk-mean enthalpy

#### NOMENCLATURE

$A_c$	cross-sectional area of duct
BFC	body fitted coordinate
$c_p$	specific heat
$C_1, C_2, C_3, C_4$	geometric coefficients
$D_h$	hydraulic diameter
$h$	enthalpy
$J$	Jacobian determinant
$k$	turbulent kinetic energy
$l$	distance along the periphery ( $\Gamma$ ) of the duct
NIST	National Institute of Standards and Technology
$Nu$	Nusselt number
$q''$	heat flux
$s, S$	source terms
SIMPLE	Semi-Implicit Method for Pressure Linked Equation
$T$	temperature
$T_w$	wall temperature
TDMA	Tri-Diagonal Matrix Algorithm
$u, v, w$	Cartesian velocity components
$U, V$	contravariant velocity components
$Y^+$	non-dimensional normal distance
$x, y, z$	Cartesian coordinates
<i>Greek Symbols</i>	
$\alpha$	convective heat transfer coefficient
$\varepsilon$	rate of dissipation of turbulent kinetic energy
$\Gamma$	diffusion coefficient
$\Gamma$	periphery of the duct
$\lambda$	thermal conductivity
$\phi$	general dependent variable
$\rho$	density
$\xi, \eta$	curvilinear coordinates

#### REFERENCES

- [1] GEN IV International Forum, 2007. GIF R&D Outlook for Generation IV Nuclear Energy Systems.
- [2] Igor L. Pioro, Hussam F. Khartabil, Romney B. Duffey, "Heat transfer to supercritical fluids flowing in channels-empirical correlations (survey)", Nuclear Engineering and Design 230 (2004) 69-91.
- [3] Igor L. Pioro, Romney B. Duffey, "Experimental heat transfer in supercritical water flowing inside channels (survey)", Nuclear Engineering and Design 235 (2005) 2407-2430.
- [4] X. Cheng, T.Schulenberg, "Heat transfer at supercritical pressures: literature review and application to an HPLWR" Wissenschaftliche Berichte, FZKA 6609, Forschungszentrum Karlsruhe (2001).
- [5] A. Yamaji, K. Kamei, Y. Oka, S. Koshizuka, "Improved core design of the high temperature supercritical-pressure light water reactor", Annals of Nuclear Energy 32 (2005) 651-670.
- [6] T. Schulenberg, J. Starflinger, J. Heinecke, "Three pass core design proposal for a high performance light water reactor", Progress in Nuclear Energy 50 (2008) 526-531.
- [7] K. Yamagata, K. Nishimawa, S. Hasegawa, T. Fujii, S. Yoshida, "Forced convective heat transfer to supercritical water flowing in tubes", International Journal of Heat and Mass Transfer 15 (1972) 2575-2593.
- [8] M. Zhao, H. Y. Gu, X. Cheng, "Experimental study on heat transfer of supercritical water flowing downward in circular tubes", Annals of Nuclear Energy 63 (2014) 339-349.
- [9] Siyu Zhang, Hanyang Gao, Xu Cheng, Zhenqin Xiong, "Experimental study on heat transfer of supercritical Freon flowing upward in a circular tube", Nuclear Engineering Design 280 (2014) 305-315.
- [10] Hideo Mori, Takenobu Kaida, Masaki Ohno, Suguru Yoshida, Yoshinori Hamamoto, "Heat transfer to supercritical pressure fluid flowing in sub-bundle channels", Journal of Nuclear Science and Technology 49 (2012) 373-383.
- [11] Yina Zhang, Chao Zhang, Jin Jiang, "Numerical simulation of heat transfer of supercritical fluids in circular tubes using different turbulence models", Journal of Nuclear Science and Technology 48 (2011) 366-373.
- [12] Maria Jaromin, Henryk Anglart, "A numerical study of heat transfer to supercritical water flowing upward in vertical tubes under normal and deteriorated conditions", Nuclear Engineering Design 264 (2013) 61-70.
- [13] Q. L. Wen, H. Y. Gu, "Numerical simulation of heat transfer deterioration phenomenon in supercritical water through vertical tube", Annals of Nuclear Energy 37 (2010) 1272-1280.
- [14] Karki, K. C. and Patankar, S. V., Calculation Procedure for Viscous Incompressible Flows in Complex Geometries, *Numerical Heat Transfer*, vol. 14, pp. 295-307, 1988a.
- [15] Melaaen, M. C., Calculation of Fluid Flows With Staggered and Nonstaggered Curvilinear Nonorthogonal Grids - The Theory, *Numerical Heat Transfer, Part B*, vol. 21, pp. 1-19, 1992a.
- [16] Shyy, W., Tong, S. S. and Correa, S. M., Numerical Recirculating Flow Calculation Using a Body-Fitted Coordinate System, *Numerical Heat Transfer*, vol. 8, pp. 99-113, 1985.
- [17] Acharya, S. and Moukalled, F. H., Improvements to Incompressible Flow Calculation on a Nonstaggered Curvilinear Grid, *Numerical Heat Transfer, Part B*, vol. 15, pp. 131-152, 1989.
- [18] Choi, S. K. and Nam, H. Y., Use of the Momentum Interpolation Method for Numerical Solution of Incompressible Flows in Complex Geometries: Choosing Cell Face Velocities, *Numerical Heat Transfer, Part B*, vol. 23, pp. 21-41, 1993.
- [19] Rhie, C. M. and Chow, W. L., Numerical Study of the Turbulent Flow Past an Airfoil With Trailing Edge Separation, *AIAA Journal*, vol. 21, pp. 1525-1535, 1983.
- [20] Launder B. E., Spalding D. B., The numerical computation of turbulent flows, *Computational Methods in Applied Mechanics and Engineering*, vol. 3, pp. 269-289, 1974.